JOURNAL OF RAMAN SPECTROSCOPY
J. Raman Spectrosc. 2008; **39**: 1170–1177
Published online 4 April 2008 in Wiley InterScience
(www.interscience.wiley.com) DOI: 10.1002/jrs.1958

JRS

Theoretical study on SERRS of rhodamine 6G adsorbed on Ag_2 cluster: chemical mechanism via intermolecular or intramolecular charge transfer

Shasha Liu,[1] Songbo Wan,[2,3] Maodu Chen[1]* and Mengtao Sun[2]*

[1] School of Chemical Engineering, School of Physics and Optoelectronic Technology and College of Advanced Science and Technology, Dalian University of Technology, Dalian 116024, PR China
[2] Beijing National Laboratory for Condensed Matter Physics, Institute of Physics, Chinese Academy of Sciences, Beijing, 100080, PR China
[3] Physical Science and Technology College, Zhengzhou University, Zhengzhou, P. R. China

Received 26 November 2007; Accepted 31 January 2008

The problem of the chemical enhancement of rhodamine 6G (R6G) adsorbed on silver cluster has been theoretically investigated by charge difference densities (CDDs) to show the direct charge transfer (CT) evidence. For surface-enhanced resonance Raman scattering (SERRS) of R6G excited at 514.5 nm, the enhancements of v(151) and v(154) result from weak intermolecular (from Ag to R6G) CT and the strong intramolecular CT [similar to that of resonance Raman scattering (RRS) of R6G], respectively. The possibility of the SERRS of R6G contributed from pure intermolecular CT is also discussed, when the incident light is close to the new metal–R6G CT excited state at 1571.4 nm. Meanwhile compared with the absorption process the fluorescence yield of R6G is investigated by transition densities and CCDs.
Copyright © 2008 John Wiley & Sons, Ltd.

Supplementary electronic material for this paper is available in Wiley InterScience at http://www.interscience.wiley.com/jpages/0377-0486/suppmat/

KEYWORDS: charge difference density; chemical mechanism via charge transfer; R6G; R6G–Ag_2 complex; SERRS

INTRODUCTION

Molecular Raman scattering can be enormously enhanced by molecules adsorbed on or near a rough metallic surface or a colloidal metallic particle surface. This phenomenon is called surface-enhanced Raman scattering (SERS) and recently evolved as a significant laser spectroscopic characterization technique.[1–7] SERS could surmount the potential high background fluorescence in normal Raman spectra and the shortcoming of low scattering cross-section.[8,9] It is generally recognized that the huge enhancement in SERS is attributed mainly to two kinds of mechanisms.[5–10] One is the electromagnetic (EM) mechanism, which is due to the strong surface plasmon resonance in curved metallic surfaces coupled to the incident light.[10–13] The other is the chemical enhancement, which is caused by metal to molecule or molecule to metal charge transfer (CT) electronic transition.[6,10,14–16] The EM mechanism can obtain an enhancement factor in the order of 10^4–10^6, while the chemical enhancement is considered to be of the order of about 10^2.[6,10,17,18]

In recent years single molecule detection has been well developed especially adopting the SERS or surface-enhanced resonance Raman scattering (SERRS) method, which has been called single molecule surface-enhanced Raman spectroscopy (SMSERS). In SMSERS, the enhancement factor can be of the order 10^{14}–10^{15}.[19] Electrodynamics calculations on dimers or triangular prisms and spherical nanoparticles have expressed that 10^{11} order of magnitude can be achieved in EM enhancement.[20,21] Nevertheless it has proved so difficult to solve the chemical contribution in SMSERS that it is still an urgent problem in this area. Owing to the significant role in surface-enhanced Raman spectroscopy, Rhodamine 6G (R6G) (Fig. 1) has been used in high sensitive detection, for instance, single molecule detection utilizing SERRS.[19–21] In visible light, the R6G cationic dye has strong absorption accompanying a severe fluorescence yield. However, the strong fluorescence yield of R6G may prevent observation of the Raman spectrum.[22]

Numerous experimental and theoretical investigations have been carried out to reveal the structural, electronic, and

*Correspondence to: Maodu Chen, School of Chemical Engineering, School of Physics and Optoelectronic Technology and College of Advanced Science and Technology, Dalian University of Technology, Dalian 116024, PR China. E-mail: mdchen@dlut.edu.cn
Mengtao Sun, Beijing National Laboratory for Condensed Matter Physics, Institute of Physics, Chinese Academy of Sciences, Beijing, 100080, PR China.

Copyright © 2008 John Wiley & Sons, Ltd.

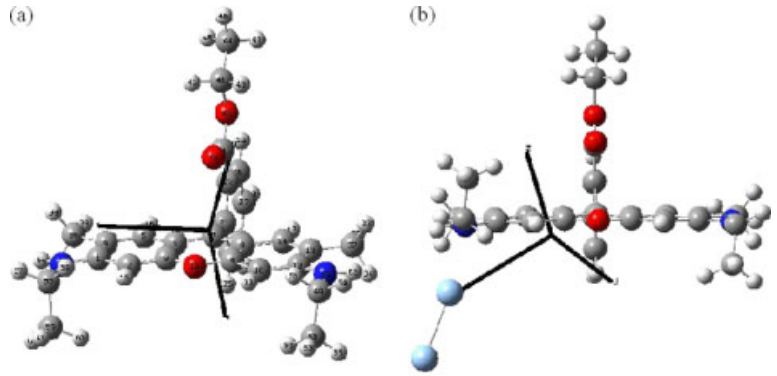

Figure 1. (a) Optimized geometry of R6G in the ground state using BP86/6–31G (d, p) level, and (b) optimized geometry of R6G–Ag_2 complex in the ground state of R6G using BP86/6–31G and LanL2DZ level for C, H, O, N and Ag atom, respectively. This figure is available in colour online at www.interscience.wiley.com/journal/jrs.

optical properties of R6G. Watanabe *et al*.[23] have compared tip-enhanced near-field Raman scattering (TERS) spectra of R6G with conventional SERRS spectra under the same conditions of excitation frequency and sample preparation. Meanwhile they have adopted density functional theory (DFT) to perform calculations of vibration and assign the vibrational modes of the R6G molecule. They have developed a technique of the tip-surface doubly enhanced near-field Raman spectroscopy to detect molecular orientations and distributions. Theoretically Jensen and Schatz[24] have preformed normal Raman scattering (NRS) and resonance Raman scattering (RRS) spectra calculations of R6G using time-dependent density functional theory (TDDFT) in their works. Calculations in RRS have shown that resonance enhancements have been found to be of the order of 10^5.

Those previous works mentioned above have provided some understanding of the enhancement of SERS or SERRS but it is easy to confuse chemical enhancement with EM mechanism in SERS or SERRS. This problem calls for a great deal of further research effort in this area. Hence, in this article we present a technique to differentiate the CT mechanism from the EM mechanism. Chemical mechanism of SERRS of R6G is under investigation while R6G is adsorbed on the metallic silver cluster. First of all the optical absorption of R6G and R6G–Ag_2 complex (Fig. 1) is discussed. At the same time the fluorescence property of R6G is calculated. Then we explain the chemical mechanism of RRS and SERRS of R6G via intermolecular and intramolecular CT. Finally we focus on the enhancement of SERRS of R6G caused by intermolecular CT.

COMPUTATIONAL METHODS

The ground state structure of R6G was optimized using DFT[25] with BP86 functional[26,27] at the level of 6–31G (d, p) basis set. The ground state structure of R6G–Ag_2 complex was optimized using DFT with BP86 functional at the level of 6–31G basis set for C, N, O, H atoms and LanL2DZ for Ag atoms, respectively.[28] There were no imaginary wavenumbers found in the wavenumber analysis. The calculations for adiabatic electronic state optical absorption of R6G and R6G–Ag_2 complex were carried out by the TDDFT method[29] using BP86 functional with the same basis set. All these calculations were performed in GAUSSIAN03 suit.[30] The excited-state geometry optimization of R6G was calculated using TDDFT method with B3LYP functional and SV (P) basis set[31] (which is approximately 6–31G*) with TURBOMOLE program.[32] With the optimized excited-state geometry, the fluorescence energy of R6G was reproduced by TDDFT method, BP86 functional at the level of 6–31G (d, p) basis set, which is calculated with GAUSSIAN03. Fluorescence was treated at the TD-BP86/6–31G (d, p)//TD-B3LYP/SV (P) level in conventional quantum-chemical notation 'single point//optimization level'.[33]

Absolute off and on resonance Raman intensities can be calculated as the differential Raman scattering cross-section. For Stokes scattering with an experimental setup of a 90° scattering angle and perpendicular planar-polarized light, the cross-section is written as[34]

$$\frac{d\sigma}{d\Omega} = \frac{\pi^2}{\varepsilon_0^2}(\omega_{in} - \omega_p)^4 \frac{h}{8\pi^2 c\omega_p} S_p \frac{1}{45[1 - \exp(-hc\omega_p/k_B T)]} \quad (1)$$

The ω_{in} and ω_p are the frequency of the incident light and of the pth vibrational mode, respectively, and S_p is the Raman scattering factor (or Raman activity in unit $Å^4$/amu),

$$S_p = 45\left(\frac{\partial \alpha_p}{\partial Q_p}\right)^2 + 7\left(\frac{\partial \gamma_p}{\partial Q_p}\right)^2 \quad (2)$$

which is a pure molecular property and independent of experimental setup. α_p and γ_p are the isotropic and anisotropic polarizabilities. In this article, S_p is directly calculated by Gaussian 03 suite.[30]

The transition density and charge difference density (CDD) were adopted to study the photoinduced excited-state properties of the R6G and the R6G–Ag_2 complex, which reveal the orientation and strength of transition dipole

Copyright © 2008 John Wiley & Sons, Ltd.

DOI: 10.1002/jrs

moments, and the orientation and result of intramolecular and intermolecular CT on the excitation, respectively.[10,35,36]

RESULTS AND DISCUSSION

Molecular geometry

We have optimized the molecular geometry of the cationic R6G in the ground state using the BP/6–1G (d, p) basis set in vacuum. There are no imaginary wavenumbers in the wavenumber analysis of the initial structure, therefore expressing an energy minimum. These geometrical data together with the 4XD parameters[37] and the calculated data by Watanabe's are listed in Table 1. Also the geometrical parameters of the excitation state R6G molecule are listed. In the crystal structure of R6G, the dihedral angle between the xanthene plane and phenyl-ring plane is 62°,

Table 1. Calculated bond lengths (in Å), bond angles (in degree), and dihedral angles (in degree) of ground state and excited state of R6G at BP/6–31G (d, p) level[a] and B3LYP/SV (P) level, respectively

	Ground state			Excited state
	4XD (exp[b])	Calculated B3LYP/6–311++ G(d,p)	Calculated BP/6–31G(d,p)	Calculated B3LYP/def-svp
		Bond length (Å)		
C1–C2	1.409	1.407	1.417	1.417
C1–C6	1.442	1.446	1.452	1.444
C1–N20	1.325	1.354	1.362	1.363
C2–C3	1.361	1.380	1.390	1.389
C3–O18	1.368	1.358	1.371	1.360
C3–C4	1.419	1.419	1.430	1.424
C4–C5	1.430	1.424	1.430	1.425
C4–C7	1.388	1.408	1.420	1.434
C5–C6	1.341	1.368	1.382	1.386
C6–C36	1.502	1.506	1.510	1.507
C7–C21	1.491	1.496	1.499	1.489
C21–C22	1.381	1.398	1.410	1.406
C21–C23	1.400	1.401	1.420	1.418
C22–C24	1.373	1.393	1.403	1.399
C23–C26	1.392	1.401	1.410	1.406
C23–C31	1.475	1.497	1.498	1.500
C24–C27	1.370	1.392	1.403	1.397
C26–C27	1.361	1.390	1.400	1.396
C31–O40	1.193	1.213	1.231	1.213
C31–O43	1.333	1.338	1.354	1.339
C41–O43	1.462	1.458	1.466	1.443
C41–C44	1.470	1.513	1.519	1.516
C49–C52	1.493	1.531	1.537	1.536
		Bond angles (°)		
C1–C6–C5	119.3	118.8	118.8	118.6
C1–C6–C36	119.8	120.0	120.0	120.3
C2–C1–C6	118.4	119.4	119.6	119.2
C2–C1–N20	122.1	121.7	121.6	121.4
C2–C3–C4	123.1	122.5	122.6	122.3
C2–C3–O18	116.6	116.7	116.3	116.2
C3–C4–C5	114.9	116.4	116.5	116.3
C3–O18–C9	120.2	121.0	120.4	120.5
C4–C5–C6	123.9	123.0	123.0	123.5
C4–C7–C21	119.7	120.4	120.4	121.3
C4–C7–C8	119.3	119.1	118.8	117.2
C5–C4–C7	125.3	124.4	124.2	124.1

(*continued overleaf*)

Copyright © 2008 John Wiley & Sons, Ltd.

DOI: 10.1002/jrs

Table 1. (*Continued*)

	Ground state			Excited state
	4XD (exp[b])	Calculated B3LYP/6−311++ G(d,p)	Calculated BP/6−31G(d,p)	Calculated B3LYP/def-svp
N20−C56−C59	112.8	113.8	113.7	114.0
C21−C22−C24	121.8	120.9	120.8	121.3
C21−C23−C26	119.3	119.4	119.7	119.7
C21−C23−C31	120.8	119.8	119.0	120.0
C22−C24−C27	119.6	120.0	120.1	119.9
C23−C26−C27	121.0	120.9	120.7	121.0
C23−C31−O40	125.2	123.7	123.8	124.3
C23−C31−O43	109.8	112.7	112.3	112.5
C24−C27−C26	120.2	119.7	119.8	119.7
C31−O43−C41	117.5	116.9	115.4	117.5
O43−C41−C44	108.7	107.6	107.4	108.0
		Dihedral angles (°)		
C2−C1−N20−C56	−2.9	−1.8	−3.9	−2.9
C1−N20−C56−C59	−118.3	−92.7	−80.5	−82.6
C4−C7−C21−C23	84.6	82.1	86.4	88.2
C10−C12−N19−C49	−0.2	1.8	3.9	2.8
C21−C23−C31−O40	35.3	0.0	0.0	−0.1
C31−O43−C41−C44	−93.6	−180.0	−180.0	−180.0

[a] Atom numbering as in Fig. 1.

[b] Experiment data in Ref. 37.

whereas the dihedral angle is 87° in our calculated geometry, which is consistent with Watanabe's results at the level of DFT-B3LYP/6−311 + +G (d, p).[23] The conformational differences in the crystal and the calculated structure owe to the packing effect in the crystal. In Tab 1e 1 it can be found that the structure of R6G optimized by the level of BP86/6−31G (d, p) in the ground state has slightly longer bond lengths than those of Watanabe *et al*. However, bond angles and dihedral angles are in good agreement with results in Ref. 23. These differences between our results and the data in Ref. 23 can be ascribed to adoption of different functionals in the calculations.

In the ground state, our calculated results of R6G show that charges on the phenyl-ring group (ethoxycarbony) are very small (0.092 e) whereas nearly all of positive charges (1 e) are localized on the xanthene plane and two NHC_2H_5 groups. For the R6G−Ag_2 complex at the ground state, the CT from the Ag_2 cluster to R6G is 0.13 e, which indicates that the interaction between R6G and the Ag_2 cluster is weak. We can consider the R6G−Ag_2 complex as a weak chemisorbed system. The static electronic polarizablity between Ag_2 and R6G is not so strong, which can be noted from the data in Table 2.

We also performed the calculation of the excited-state molecular geometry of R6G by the level of B3LYP/SV (P) using TURBOMOLE program. As shown in Table 1, it is easy to find there are no obvious differences in geometries between the excited state and the ground state of R6G. The dihedral angle between the xanthene plane and phenyl-ring plane is 86° in the excited state, whereas the dihedral angle is 87° in ground state.

Table 2. The static electronic polarizability of R6G and R6G−Ag2 complex, the unit is atomic unit (a.u.). Their Cartesian coordinates are in Fig. 1

	xx	xy	yy	yz	zx	zz
R6G	573.638	−0.034	414.565	0.010	41.267	261.638
R6G−Ag_2	852.284	−84.447	506.473	4.249	14.876	391.077

Absorption spectra and fluorescence properties

Our calculated optical absorption spectra of R6G and R6G−Ag_2 are listed in Fig. 2. The results indicate that the S_1 electronic state transition of R6G in vacuum is 474.53 nm with strong oscillator strengths ($f = 0.59$), which is about 50 nm blue-shifted from the main electronic absorption ($\lambda_{max} \approx 520$ nm) of R6G in ethanol solution. In Ref. 23, the transition energy is 2.62 eV (474 nm) for S_0-S_1 adopting the BP86 functional. They found that in aqueous solution the excitation energy was 2.44 eV (508 nm) which is in better agreement with the experimental result. So, the discrepancy between our calculated optical spectra and the experimental result is mainly due to the neglect of the solvent effect in the

Copyright © 2008 John Wiley & Sons, Ltd.

DOI: 10.1002/jrs

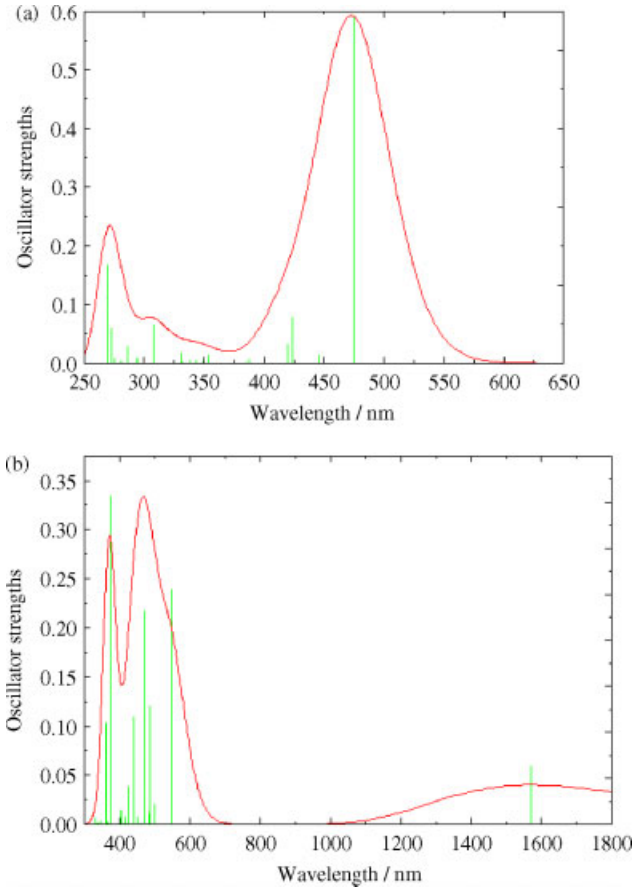

Figure 2. (a) The calculated absorption spectrum of R6G at the level of BP86/6−31G (d, p) in vacuum, and (b) the calculated absorption spectrum of R6G−Ag_2 complex at the level of BP86/LanL2DZ for Ag and 6−31G for other atoms, respectively. This figure is available in colour online at www.interscience.wiley.com/journal/jrs.

calculation. It will be a time-consuming work to consider the solvent effect which is not a decisive factor, so we ignore it in our calculation.

Due to the nature of the interaction between R6G and the Ag_2 cluster, new CT excited states would emerge in the R6G−Ag_2 complex. The calculated optical absorption spectrum of R6G−Ag_2 is shown in Fig. 2. The S_1 electronic state transition of the complex is red-shifted to 1571.4 nm with weak oscillator strength ($f = 0.059$), which is much more red-shifted than Zhao's results (1010 nm).[38] This great discrepancy is caused by the significant difference in the molecular geometry. For our result the distance between the N atom of R6G and the Ag atom is 2.51 Å, whereas the distance is 3.08 Å in Zhao *et al.*'s calculation.[38] It is reckoned that the problem could be interpreted in the light of adopting different basis sets which have great influence on calculated molecular geometry. The orbital transition for the S_1 excited state is from HOMO to LUMO. The effect of the Ag_2 cluster on R6G lead to a red shift of the main transition to 547.4 nm, which is a 25-nm shift compared to that in ethanol solution, whereas it is consistent with the main transition in Zhao *et al.*'s results (544 nm).[38]

It is well known that the fluorescence yield of R6G which would disturb the signal of the Raman spectrum is strong in visible light. The optimized fluorescence energy of R6G shows the fluorescence absorption in 483.45 nm (2.5646 eV, $f = 0.58$) at the level of BP86/6−31G (d, p) which is slightly less than the absorption maximum of R6G in energy (474.53 nm, 2.613 eV, $f = 0.59$ by the level of BP86/6−31G (d, p)). We show the transition densities and the CDDs of the R6G in both absorption and fluorescence process in Table 3. The calculated S_1 transition dipole moments in absorption and fluorescence are listed in Table 4. It can be found that the orientation of the transition dipole moment is consistent with the orientation of the transition density. Comparing the transition densities of R6G in absorption and that in the fluorescence process, it is easy to find that they are consistent with each other. Both of them are due to the process of charges transfer from the right side of xanthene to the left side of xanthene in R6G, since the electrons and holes are totally localized on left and right side xanthene, respectively. However, we can find that there are obvious differences in the CDDs of R6G (Table 3) in the absorption process by contrast with that in the fluorescence process, since the electrons and holes are localized on completely reverse position. That is, the transferred electrons on the absorption will move back on the fluorescence. This is the most important difference between absorption process and fluorescence property.

NRS and SERRS spectrum of R6G and R6G−AG_2 complex

The experimental and theoretical normal Raman spectra of R6G which have a good agreement with each other are listed in Fig. 3(a) and (b). We focus on several normal modes with

Table 3. The transition and charge difference densities of R6G. Green color represents the hole and red color the electron. The isovalue is 2×10^{-4} in a.u

	Transition density	Charge difference density
Absorption (S_1)		
Fluorescence (S_1)		

Copyright © 2008 John Wiley & Sons, Ltd.

Table 4. The transition dipole moments of R6G in absorption and fluorescence, the unit is atomic unit (a.u.). Their Cartesian coordinates are in Fig. 1

	Absorption			Fluorescence		
S_1	−3.0375	−0.0007	0.0000	−3.0381	0.0189	−0.0008

high intensity all of which are the symmetric vibration on the xanthene ring and/or the NHC2H5 group.

According to the theoretical NRS and experimental RRS in Fig. 3(b) and (c), we find from 600 cm^{-1} to 1400 cm^{-1} the profiles of them are identical in principle. However, in the range of 1400–1800 cm^{-1} the relative intensity of RRS is obviously increased, which is thought to be the effect of the chemical mechanism via intramolecular CT. In this special area, the vibrational mode of $v(154)$ is a complete C═C symmetric stretching mode of the xanthene ring (Fig. 1S, Supplementary Material). The reason why the normal mode $v(154)$ is strongly enhanced is electron transfer from the edge of the xanthene ring to the inner of the xanthene ring, which results from the HOMO to LUMO orbital transition. The normal mode $v(151)$ is the C═C symmetric stretching of the phenyl ring (Fig. 1S). The

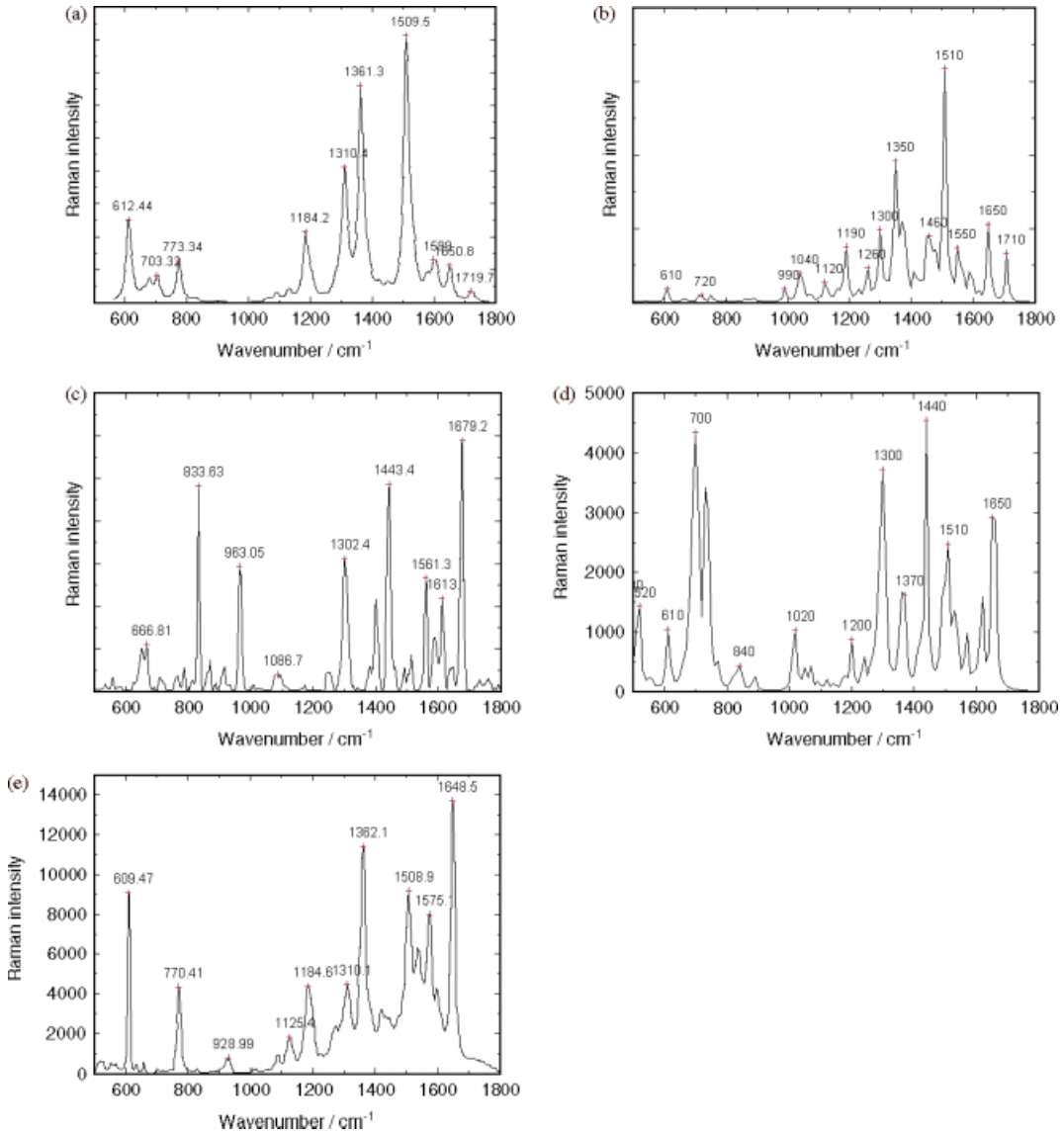

Figure 3. (a) Experimental off-resonance Raman spectrum of R6G in ethanol solution (Ref. 23), (b) the calculated normal Raman spectrum of R6G at zero frequency, (c) the resonance Raman spectrum of R6G in 488 nm (Ref. 23), (d) the calculated normal Raman spectrum of R6G–Ag_2 complex at zero frequency, (e) relative intensities of calculated Raman spectrum of R6G constructed from the data reported in Table 3 of Ref. 23, and broadened with a Lorentzian line profile having a width of 20 cm^{-1}. This figure is available in colour online at www.interscience.wiley.com/journal/jrs.

Copyright © 2008 John Wiley & Sons, Ltd.

DOI: 10.1002/jrs

explanation for the strongly enhanced intensities of $v(151)$ is that the electron transfer from the xanthene plane to the phenyl ring, which contributed from the $H-1$ to $L+2$ orbital transitions. Consequently, the chemical enhancement of R6G in RRS is the result of the intramolecular CT.

Comparing the experimental SERRS of R6G with the calculated NRS of the R6G–Ag_2 complex in Fig. 3(d) and (e), it is easy to find that there is no great difference between the profiles. In our model, we considered only the chemical interaction between R6G and Ag atoms. For the SERRS of R6G, the vibrational modes of $v(154)$ and $v(151)$ are strongly enhanced compared to the NRS of R6G. The strong enhancement of these two modes result from the weak intermolecular electrons transfer from Ag_2 cluster to R6G and strong intramolecular electron transfer in R6G, including the electron transfer from the edge of xanthene ring to the inner of the xanthene ring, and electron transfer from xanthene plane to phenyl ring.

The central theories of chemical enhancement is to invoke RRS by a CT intermediate state. Adsorbed molecular orbitals are extended into resonances by interaction with the conduction electrons. There are two probabilities for new excitations: One is molecule–metal CT: during this process electrons can be excited from the fully filled molecular orbitals to empty metal orbitals; the other is metal–molecule CT in which metal electrons can be excited to the partially filled molecular orbitals. From the CDDs in Table 1S (Supplementary Material), there are seven CT excited states, where the electrons excited on the Ag_2 are transferred to R6G. Due to CT for these excited states, the holes are localized on the Ag_2 cluster while all electrons are localized on R6G. It is clear that electrons are excited from the metal to the adsorbed molecule. The chemical mechanism of SERRS is considered similar to a resonance Raman process between the ground electronic state of the molecule–metal complex and its new excited levels arising from CT between the metallic surface and the adsorbed molecule. So we afford a direct theoretical evidence for chemical mechanism of SERRS by providing visualized CT between R6G and Ag_2 cluster with CDD.

In Table 5 seven excited states S_1, S_6, S_8, S_9, S_{18}, S_{19}, S_{26} are complete CT (between R6G and the Ag_2 cluster) with weak oscillator strengths. The first transition in 1571.4 nm of all these excited states has the largest oscillator strengths ($f = 0.0590$). Notice that there is no intramolecular (R6G) CT in S_1. Therefore, the chemical enhancement of SERRS of R6G at the incident light of 1571.4 nm should be via pure intermolecular CT (from Ag_2 cluster to R6G). That is in 0.7890 eV (1571.40 nm), when the excitation wavelength is resonant with this CT excited state, there should be the strongest chemical enhancement to SERRS. Considering other pure CT excited states in Table S1 when the excitation wavelength is resonant with those CT excited states, respectively, there also should be chemical enhancement with smaller contribution to SERRS.

Table 5. The charge difference density of the R6G–Ag_2 complex for the seven pure charge transfer (CT) states. Green color represents the hole, red color the electron. The isovalue is 2×10^{-4} in a.u

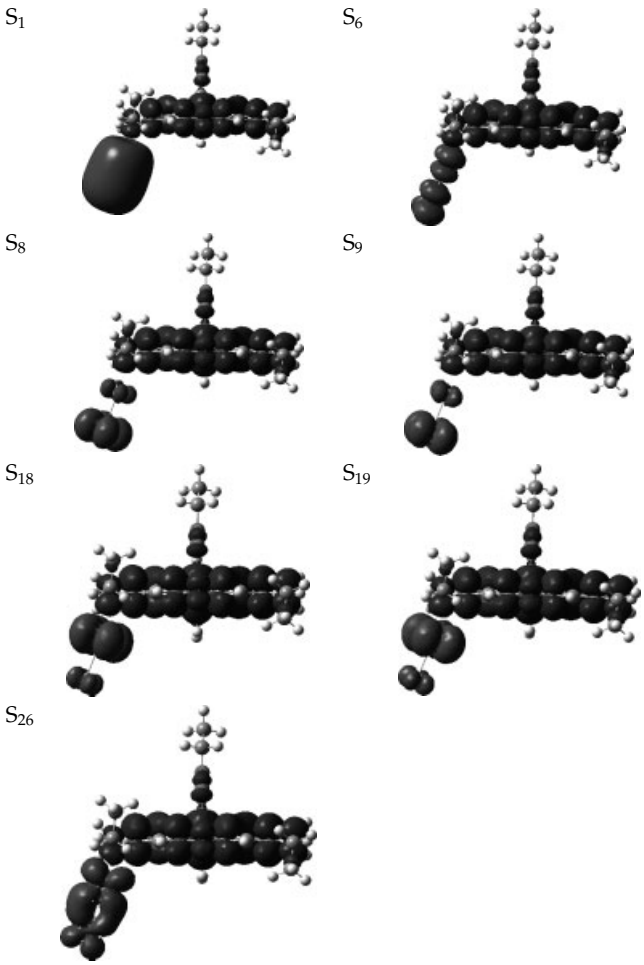

Actually the calculated excited states of the R6G–Ag_2 complex S_3, S_7, S_{11} and S_{12} (Table S1) are CT states with strongest oscillator strengths; however, in these excited states there is not only involving charge transition from the Ag_2 cluster to R6G but also including intramolecular CT of R6G. That means when the excitation wavelength is resonant with these CT excited states, there should be strongest chemical enhancement contributed by RRS and SERRS together. Especially, we pay more attention to S_3 (547.39 nm $f = 0.2395$) with the strongest oscillator strengths since it plays a primary role in SERRS. Notice that S_{16}, S_{17} and S_{22} are totally intramolecular CT of R6G without participation of the Ag_2 cluster, furthermore almost all the holes are localized on the carboxyphenyl group and nearly all the electrons are localized on the xanthene chromophore and the nitrogen of the ethylamino group. This can be explained that the chemical enhancement roots in RRS of R6G when the excitation wavelength is resonant with these

Copyright © 2008 John Wiley & Sons, Ltd.

DOI: 10.1002/jrs

CT excited states. Finally there is a novel phenomenon in the last transition of R6G S_{30} (331.80 nm $f = 0.0064$) which the charges transfer from R6G to Ag_2 cluster. In this excited state all the holes are localized on the R6G and all the electrons are localized on the Ag_2 cluster.

CONCLUSIONS

In summary we have provided direct CT evidence by CDDs to show theoretically the chemical enhancement of R6G adsorbed on silver. In visualization ways we investigate how CT occurs in the R6G–Ag_2 complex and within R6G with CDD, which shows visually the orientation and result of CT in photoinduced dynamics. The CT in R6G and the R6G–Ag_2 complex is considered as the evidence for chemical enhancement in RRS and SERRS. For SERRS of R6G excited at 514.5 nm, the enhancements of v(151) and v(154) result from weak intermolecular (from Ag to R6G) CT, and the strong intramolecular CT (similar to that of RRS of R6G). The possibility of the SERRS of R6G contributed from pure intermolecular CT is also discussed, when the incident light is close to the new metal-R6G CT excited state at 1571.4 nm.

Supplementary material

Supplementary electronic material for this paper is available in Wiley InterScience at: http://www.interscience.wiley.com/jpages/0377-0486/suppmat/

Acknowledgements

We thank Prof. Keli Han for helpful discussions. This work was supported by the National Natural Science Foundation of China (Grant Nos. 10604012 and 20703064), the National Basic Research Project of China (Grant No. 2007CB936804), and SRF for ROCS, SEM (2006).

REFERENCES

1. Jeanmaire DL, Van Duyne RP. *J. Electroanal. Chem.* 1977; **84**: 1.
2. Albrecht MG, Creighton JA. *J. Am. Chem. Soc.* 1977; **99**: 5215.
3. Moskovits M. *Rev. Mod. Phys.* 1985; **57**: 783.
4. Kneipp K, Kneipp H, Itzkan I, Dasari RR, Feld MS. *Chem. Rev.* 1999; **99**: 2957.
5. Otto A, Grabhorn H, Akemann W. *J. Phys. Condens. Matter.* 1992; **4**: 1143.
6. Campion A, Ivanecky JE, Child CM III, Foster M. *J. Am. Chem. Soc.* 1995; **117**: 11807.
7. Lombardi JR, Birke RL, Lu T, Xu J. *J. Chem. Phys.* 1986; **84**: 4174.
8. Xu HX, Bjerneld EJ, Kall M, Borjesson L. *Phys. Rev. Lett.* 1999; **83**: 4357.
9. Xu HX, Wang XH, Persson MP, Xu HQ. *Phys. Rev. Lett.* 2004; **93**: 243002.
10. Sun MT, Wan SB, Liu YJ, Yu J, Xu HX. *J. Raman Spectrosc.* 2008; **39**: 402.
11. Draine BT, Flatau PJJ. *Opt. Soc. Am. A.* 1994; **11**: 1491.
12. Jensen T, Kelly L, Lazarides A, Schatz GC. *J. Cluster. Sci.* 1999; **10**: 295.
13. Xu HX, Käll M. *Phys. Rev. Lett.* 2002; **89**: 246802.
14. Zhao LL, Jensen L, Schatz GC. *Nano Lett.* 2006; **6**: 1229.
15. Zhao LL, Jensen L, Schatz GC. *J. Am. Chem. Soc.* 2006; **128**: 2911.
16. Jensen L, Zhao LL, Schatz GC. *J. Phys. Chem. C.* 2007; **111**: 4756.
17. Futamata M, Maruyama Y. *Anal. Bioanal. Chem.* 2007; **388**: 89.
18. Michaels AM, Nirmal M, Brus LE. *J. Am. Chem. Soc.* 1999; **121**: 9932.
19. Nie S, Emory SR. *Science.* 1997; **275**: 1102.
20. Kneipp K, Wang Y, Kneipp H, Perelman LT, Itzkan I, Dasari RR, Feld MS. *Phys. Rev. Lett.* 1997; **78**: 1667.
21. Michaels AM, Jiang J, Brus L. *J. Phys. Chem. B.* 2000; **104**: 11965.
22. Hibara A, Saito T, Kim HB, Tokeshi M, Ooi T, Nakao M, Kitamori T. *Anal. Chem.* 2002; **74**: 6170.
23. Watanabe H, Hayazawa N, Inouye Y, Kawata S. *J. Phys. Chem. B.* 2005; **109**: 5012.
24. Jensen L, Schatz GC. *J. Phys. Chem. A.* 2006; **110**: 5973.
25. Hohenberg P, Kohn W. *Phys. Rev.* 1964; **136**: B864.
26. Becke AD. *Phys. Rev. A.* 1988; **38**: 3098.
27. Perdew JP. *Phys. Rev. B.* 1986; **33**: 8822.
28. Hay PJ, Wadt WR. *J. Chem. Phys.* 1985; **82**: 270.
29. Gross EKU, Kohn W. *Phys. Rev. Lett.* 1985; **55**: 2850.
30. Frisch MJ, Trucks GW, Schlegel HB, Scuseria GE, Robb MA, Cheeseman JR, Montgomery Jr., JA, Vreven T, Kudin KN, Burant JC, Millam JM, Iyengar SS, Tomasi J, Barone V, Mennucci B, Cossi M, Scalmani G, Rega N, Petersson GA, Nakatsuji H, Hada M, Ehara M, Toyota K, Fukuda R, Hasegawa J, Ishida M, Nakajima T, Honda Y, Kitao O, Nakai H, Klene M, Li X, Knox JE, Hratchian HP, Cross JB, Bakken V, Adamo C, Jaramillo J, Gomperts R, Stratmann RE, Yazyev O, Austin AJ, Cammi R, Pomelli C, Ochterski JW, Ayala PY, Morokuma K, Voth GA, Salvador P, Dannenberg JJ, Zakrzewski VG, Dapprich S, Daniels AD, Strain MC, Farkas O, Malick DK, Rabuck AD, Raghavachari K, Foresman JB, Ortiz JV, Cui Q, Baboul AG, Clifford S, Cioslowski J, Stefanov BB, Liu G, Liashenko A, Piskorz P, Komaromi I, Martin RL, Fox DJ, Keith T, Al-Laham MA, Peng CY, Nanayakkara A, Challacombe M, Gill PMW, Johnson B, Chen W, Wong MW, Gonzalez C, Pople JA. *Gaussian 03, Revision E.0.1*, Gaussian, Inc.: Wallingford CT, 2004.
31. Schäfer A, Horn H, Ahlrichs R. *J. Chem. Phys.* 1992; **97**: 2571.
32. Ahirichs R, Bär M, Baron HP, Bauernschmitt R, Böcker S, Deglmann P, Ehrig M, Eichkorn K, Elliott S, Furche F, Haase F, Häser M, Horn H, Hättig C, Huber C, Huniar U, Kattannek M, Köhn A, Kölmel C, Kollwitz M, May K, Ochsenfeld C, Öhm H, Patzelt H, Rubner O, Schäfer A, Schneider U, Sierka M, Treutler O, Unterreiner B, Arnim M, Weigend F, Weis P, Weiss H. *Turbomole 5.71; The Quantum Chemistry Group*. University of Karlsruhe: Karlsruhe, Germany, 2005.
33. Katan C, Terenziani F, Mongin O, Werts MHV, Porres L, Pons T, Mertz J, Tretiak S, Blanchard-Desce M. *J. Phys. Chem. A* 2005; **109**: 3024.
34. Neugebauer J, Reiher M, Kind C, Hess BA. *J. Comput. Chem.* 2002; **23**: 895.
35. Beenken WJD, Pullerits T. *J. Phys. Chem. B.* 2004; **108**: 6164.
36. Sun MT, Kjellberg P, Beenken WJD, Pullerits T. *Chem. Phys.* 2006; **327**: 474.
37. Adhikesavalu DN, Mastropaolo D, Camerman A, Camerman N. *Acta Cryst.* 2001; **C57**: 657.
38. Zhao J, Jensen L, Sung JH, Zou SL, Schatz GC, Van Duyne RP. *J. Am. Chem. Soc.* 2007; **192**: 7647.

Copyright © 2008 John Wiley & Sons, Ltd.